Molecular Origin of Distinct Hydration Dynamics in Double Helical DNA and RNA Sequences

Elisa Frezza, Damien Laage, Elise Duboué-Dijon

Molecular Origin of Distinct Hydration Dynamics in Double Helical DNA and RNA Sequences

Elisa Frezza,[†] Damien Laage,[‡] and Elise Duboué-Dijon[*,¶]

[†]*Université Paris Cité, CiTCoM, Paris, France*

[‡]*PASTEUR, Department of Chemistry, École Normale Supérieure-PSL, Sorbonne Université, CNRS, Paris 75005, France*

[¶]*Université Paris Cité, CNRS, Laboratoire de Biochimie Théorique, 13 rue Pierre et Marie Curie, 75005, Paris, France*

E-mail: elise.duboue-dijon@cnrs.fr

Abstract

Water molecules are essential to determine the structure of nucleic acids and mediate their interactions with other biomolecules. Here, we characterize the hydration dynamics of analogous DNA and RNA double helices with unprecedented resolution and elucidate the molecular origin of their differences: first, the localization of the slowest hydration water molecules—in the groove in DNA, next to phosphates in RNA— and second, the markedly distinct hydration dynamics of the two phosphate oxygen atoms O_R and O_S in RNA. Using our Extended Jump Model for water reorientation, we assess the relative importance of previously proposed factors, including the local topography, water bridges and the presence of ions. We show that the slow hydration dynamics at RNA O_R sites is not due to bridging water molecules, but is caused by both the larger excluded volume and the stronger initial H-bond next to O_R, due to the different phosphate orientations in A-form double helical RNA.

TOC Graphic

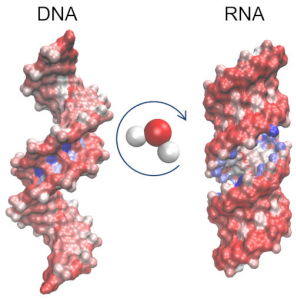

Water molecules are essential to determine the structure of nucleic acids,[1,2] with e.g. DNA conformation changing in dehydrated conditions,[3] and tightly bound structural water molecules identified in numerous RNA structures.[4–7] Trapped water molecules have been suggested to be essential for the structural dynamics and function of a ribozyme,[8] and RNA-drug interactions are mediated by long-lived water molecules.[9] More generally, water molecules in the hydration layer of nucleic acids are displaced during the formation of complexes between nucleic acids (DNA or RNA) and proteins or small drugs, and thus, are a central player in numerous biochemical recognition processes.[10–12] Hence, it is essential to understand how the properties of the hydration layer differ from those of bulk water, and to pinpoint the molecular-level determinants of their dynamics.

DNA hydration structure and dynamics have thus been extensively studied, both experimentally—with X-ray,[13,14] neutron scattering,[15] NMR,[16–19] and ultrafast spectroscopy[20–22]—and with molecular dynamics simulations.[23–27] The picture emerging from those studies is that of a strong spatial heterogeneity in the hydration dynamics with a very modest slowdown with respect to the bulk in most of the hydration shell, and very long lived water molecules in specific confined environments, such as narrow minor grooves. Some of us have shown[28] that this spatial heterogeneity can be quantitatively explained at the molecular level by the heterogeneity in both chemical composition and surface topography (i.e., the presence of more or less confined sites at the DNA surface).

In contrast, RNA solvation has been much less studied, especially its dynamics. From a structural point of view, X-ray scattering experiments[1,29–31] have identified hydration sites—phosphate groups being the most hydrated, followed by the ribose oxygen—and typical hydration structures. Double-stranded RNA (ds-RNA), which differs from DNA only by its ribose sugar instead of a deoxyribose and the nature of one of its nucleobases (U instead of T), is found in solution as A-form duplexes, strikingly different from the B-form adopted by ds-DNA (see SI Fig. S1) In this A-form, neighbor phosphate groups along each strand are closer than in the B-form, which allows the formation of single water bridges between

phosphate groups.[1,31] Bridges between phosphate and solvent-exposed nucleobase atoms have also been identified.[1] The 2′-hydroxyl group, typical of the ribose ring, has been under special focus, with water molecules suggested to form bridges between the 2′-OH and phosphate or base atoms.[29–31] However, while early studies suggested the 2′-OH group to be involved in long-lived water bridges,[31–33] molecular dynamics simulations showed that there is no long lived hydrogen-bond between water and the 2′-OH group, and that water molecules with long residence times (up to several hundreds of ps) are found instead next to the phosphate oxygen atoms,[34–38] with long-lived water bridges between successive O_R phosphate oxygen atoms. More recently, molecular dynamics simulations have shed light on the solvation dynamics of specific RNA sequences and folds,[9] such as ribozymes and riboswitches,[6,8,39] rRNA,[5,40] and RNA kinck turns,[41] identifying different solvation patterns associated with different conformations and finding a few very long lived hydration water molecules in specific, buried locations.

However, a general understanding of the molecular features that govern DNA and RNA hydration dynamics and that explain their differences has remained elusive. The broad variety of RNA folds makes it difficult to draw general conclusions on RNA hydration and the extent of its differences with that of DNA from these studies on specific sequences. Hence, in this work, we compare RNA and DNA hydration reorientation dynamics using short model double-stranded sequences adopting the typical helical conformations (A-form for RNA, B-form for DNA), and obtain for the first time a picture of the hydration dynamics at a single-site resolution. Combining our simulations with an analytic model to describe the mechanism of water reorientation and the impact of a biomolecular interface, we then provide an unprecedented molecular level rationalization of the main differences between ds-DNA and ds-RNA hydration dynamics.

We performed 100 ns-long molecular dynamics (MD) simulations of two 18-mers (GCGCGCGCGCGCGCGGC and GCGGGGGGGGGGGGGGGC, later named "GCGC" and "GGGG"), based on the systematic study conducted by the ABC consortium,[42] using the

Amber force field for nucleic acids in its parmbsc0 version[43] with χ_{OL3} modifications for RNA molecules,[44] and SPC/E water molecules.[45] Following the same strategy as in previous works by Auffinger and Westhof,[37] we chose the 18-mers to contain only GC base pairs, so that the only chemical difference between the DNA and RNA systems is the sugar—ribose in RNA and deoxyribose in DNA. The preparation of the systems, simulation setup and structural analysis are detailed in Supporting Information.

Despite very similar chemical compositions, the ds-DNA and ds-RNA 18-mers adopt strikingly different helical conformations (Figure 1 and S1). Consistently with previous structural studies, the simulated DNA B-form helices have a very narrow minor groove (width around 7.5 Å), while the major groove is much wider (see SI Figures S3-S4 and Table S1). In contrast, for the RNA A-helix, the major groove is narrow (width around 6 Å) and very deep (typical depth of about 10 Å), whereas the minor groove is wide (width around 10 Å) and shallow.

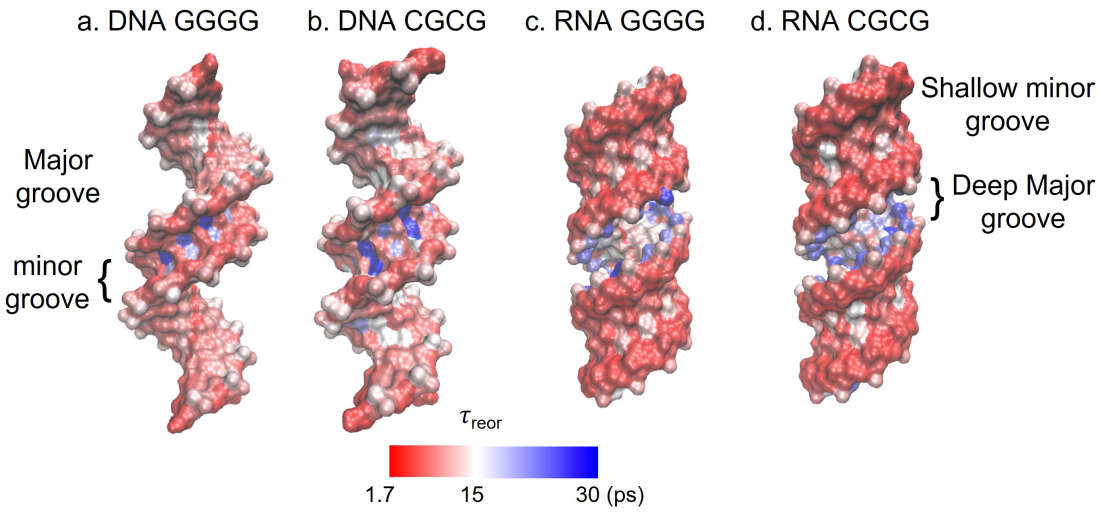

Figure 1: Maps of the site-resolved reorientation time τ_{reor} for water molecules in the hydration shell of a) DNA GGGG, b) DNA CGCG, c) RNA GGGG, and d) RNA CGCG sequences. The surface of the nucleic acid is colored according to the τ_{reor} value computed at each site. Snapshots were prepared using the VMD software.[46]

Following a strategy previously successfully applied to proteins and DNA,[28,47,48] we performed a site-resolved analysis of water dynamics in the hydration shell of these RNA and

DNA 18-mers. Water dynamics in biomolecular hydration shells can be monitored in different ways. Commonly used residence times focus on the time spent by water molecules in the vicinity of a given solute site. However, such times can only be probed indirectly in the experiments and very sensitively depend both on the exact site definition and on the time allowed for transient excursions outside the site.[49] Here, we rather focus on water reorientation dynamics, which is measurable by NMR.[50] This rotational dynamics is very closely linked to the reorganization dynamics of the H-bond network,[51,52] and thus reports on the lability of the hydration shell.

Water molecules were assigned to the nucleic acid hydration shell and to specific sites on the biomolecule following simple geometric criteria (see details in SI). Site-resolved hydration reorientation dynamics was then quantified with the reorientation time τ_{reor}, obtained by numerical integration of the reorientation time-correlation function averaged over the ensemble of water molecules initially assigned to each site. The retardation factor ρ_{reor} quantifies the slowdown in hydration dynamics with respect to the bulk.

This strategy allowed us to obtain spatially resolved maps of hydration dynamics of the DNA and RNA double helices under study (Figure 1). While earlier simulation studies, with limited statistics, relied on averaging water dynamics over equivalent sites in different base pairs along the sequence,[37,38] our simulations are long enough to allow examination of converged dynamical properties at a single-site level, as demonstrated by the estimated error bars associated with the computed single-site jump and reorientation times (see SI), that are much smaller than the variations that we will discuss.

The hydration dynamics of both DNA and RNA helices present common features. They are spatially very heterogeneous: while most of the hydration shell water molecules, in solvent-exposed sites, are only moderately slowed down compared to bulk water ($\tau_{reor} < 10\,\mathrm{ps}$, i.e. $\rho_{reor} < 6$), water molecules located in the narrow grooves (DNA minor groove and RNA deep major groove) exhibit a dynamics up to 15-20 times slower than the one observed in the bulk. These findings are consistent, for DNA, with NMR MRD measurements[18] that

evidenced a moderate 6-fold slowdown in most of the hydration shell, and the presence of a few water molecules in the grooves with longer $\sim$ 200 ps residence times. It contrasts with the bulk-like diffusion dynamics suggested by Overhauser effect dynamic nuclear polarization, which provides an estimate of the translational dynamics of water molecules within about 10 Å of the probe.[19] The discrepancy between these recent experiments and other experimental and computational techniques[53] still remains to be explained, and could be related either to the impact of the probe on water dynamics, or to some assumptions used in the model to interpret the data. Interestingly, as noted in earlier computational studies,[37,38] the location of the slowest water molecules differs between DNA and RNA sequences: in DNA, they are found at the floor of the groove, where they are H-bonded to DNA bases, whereas in RNA they lie on the side of the major groove, next to the phosphate groups.

However, the spatial resolution of such maps is limited by the diffusion of water molecules away from their initial location during the time course of the reorientation TCF calculation. A better resolution is offered by the examination of H-bond jump times, which also allows examining the molecular determinants of the hydration dynamics spatial heterogeneity. As previously shown,[51,52] water reorientation occurs mainly through large angular jumps that occur during exchanges of H-bond partner.[28,47,54,55] Since a water molecule needs to exchange H-bond acceptor to move away from an initial H-bond acceptor site on the DNA or RNA surface, the jump time (see Supporting Information) reports on the H-bond dynamics at a very well defined location, or "site". Maps of the jump times on the nucleic acids surface (see SI Fig. S9) show very similar characteristics as that of reorientation times, confirming indirectly that the jump is indeed the main ingredient of water reorientation in the hydration shell.

To gain further insight into the spatial heterogeneity and examine the impact of different features of the DNA/RNA environment on the hydration dynamics, we split the overall jump time distributions (Figure S7) according to the nature of the nearby nucleic acid site: H-bond acceptor sites (e.g., phosphate groups, O or N atoms on the base), H-bond donor sites (e.g.,

ribose OH groups), and hydrophobic groups (e.g., -CH_2- groups). In line with the findings from earlier studies on proteins and DNA,[47,54] the main peak of the jump time distributions is located at around $\tau_{jump} \simeq 6 - 7\,\mathrm{ps}$, only moderately slowed down with respect to bulk water $\tau_{jump}^{bulk} \simeq 2.5\,\mathrm{ps}$ (*i.e.* a retardation factor of about $\rho_{jump} = 2.5 - 3$), and mostly comes from water molecules located next to the biomolecule hydrophobic and H-bond donor groups (Figure 2a). We specifically examined the hydration dynamics of the ribose 2′OH group in RNA, where early structural studies have suggested long-lived hydration patterns,[31–33] that were not observed in subsequent molecular dynamics studies.[34–36] Our simulations show no sign of long-lived hydration patterns, and the hydration dynamics at these sites is only moderately slowed down, with a jump time of about 5–6 ps (*i.e.* $\rho_{jump} = 2 - 2.5$).

We now focus on the sites with slower hydration dynamics, where differences between DNA and RNA hydration dynamics are the most pronounced. In DNA, the tail of the jump time distribution is exclusively associated with water molecules next to H-bond acceptor groups on the bases in the minor groove: G(N3), with τ_{jump} ∼18–20 ps, and C(O2), with the slowest timescales, τ_{jump} ∼24–31 ps. In contrast, these sites have a much faster hydration dynamics in RNA (τ_{jump} ∼9–10 ps) and the slow jump times (τ_{jump} >20 ps) are linked to water molecules hydrating the phosphate backbone. Another striking feature is that the jump time distributions in RNA exhibit two distinct peaks, associated with phosphate hydration, at 17 ps and at nearly 30 ps, while the corresponding peaks in DNA are much closer around 15 and 19 ps (Figure 2b). More specifically, the peak corresponding to water with slower dynamics is associated with the pro-S_p phosphate oxygen atom hydration ("O_S") in DNA, whereas the characteristically slowed down water molecules in RNA (peak around 30 ps) are part of the hydration of the pro-R_p ("O_R") phosphate oxygen.

This split between RNA phosphate O_R and O_S hydration dynamics has been noticed in previous works,[34,37,38] with, however, very long residence times, of respectively 500 and 700 ps for phosphate O_S and O_R, two orders of magnitude slower than our jump times. This apparent discrepancy originates from the different probes of water hydration dynamics.

While we report reorientation times (in agreement with NMR) and H-bond exchanges, these earlier works consider residence times—which rely on criteria (e.g., site definition, treatment of transient escapes) that can significantly affect the results[49]—and report the longest time observed during their simulation. The distributions of H-bond lifetimes computed on our RNA GGGG trajectory for the O_S and O_R sites (see SI Figure S11) present a very long exponential tail, as expected for a Poisson process. The longest observed lifetimes depend on the simulation length: the longer the simulation, the more likely it is that a rare long-lived H-bond is observed. In our simulations, they are around 250 ps for O_S, and over 550 ps for O_R, even if the characteristic timescale associated with the jump dynamics at these sites is much shorter $\sim$ 30 ps. We therefore focus on the characteristic jump times instead of the longest residence times which are simulation length dependent and report only on rare events.

All the key identified features—overall shape of the jump time distributions, nature of the sites with slowest dynamics, split in hydration dynamics of RNA phosphate oxygens—are very similar in the two studied sequences, GGGG and GCGC (see Fig. 2 and Fig. S8). The average jump time at key hydration sites (e.g., 2′OH, phosphate O_S and O_R) is identical in both sequences within the computed error bars (see SI)). Interestingly, the only significant difference with alternating base pairs is observed at the slow O2(C) on the floor of the DNA minor groove, with an average jump time of 24.4 $\pm$ 1.1 ps in GGGG and 31.2 $\pm$ 2 ps in GCGC. This sequence dependence of the dynamics at slow sites in the groove is here specific to DNA, which is consistent with previous work.[38]

The slow hydration sites, phosphate groups and the floor of narrow grooves are also key interaction sites with ions and proteins, and thus often involved in the formation of protein-nucleic acid complexes and drug binding events. We thus want to go beyond the high-resolution site-level characterization of differences between DNA and RNA hydration dynamics. We now seek a physical understanding of the molecular origin of these differences, focusing on the slow sites and starting with phosphate hydration, where we found distinctly

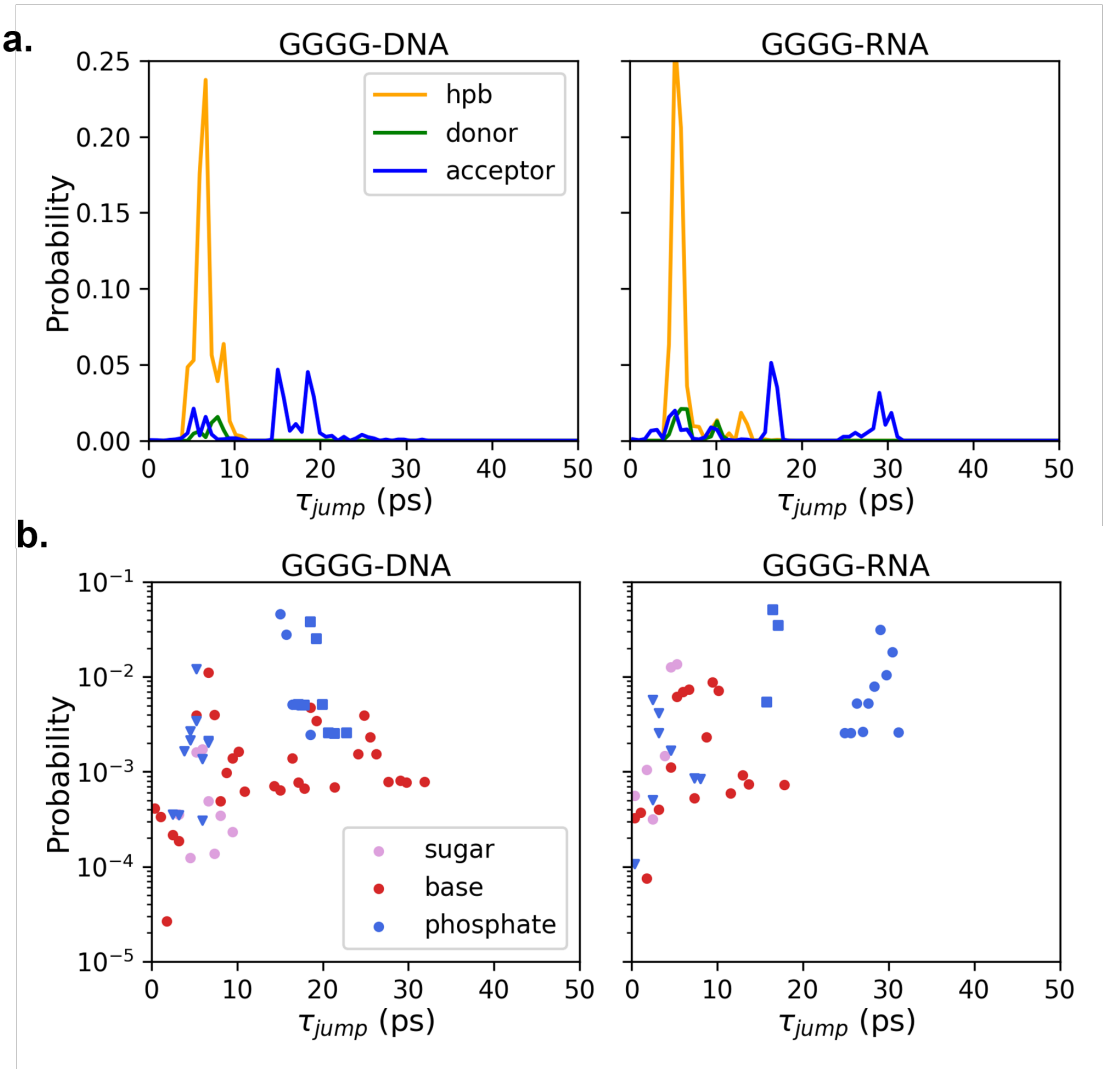

Figure 2: a) Distributions of jump time τ_{jump} for water molecules in the hydration shell of both DNA- and RNA- GGGG sequences, decomposed into contributions from water molecules assigned to hydrophobic sites ("hpb", orange), H-bond donor sites (green), and H-bond acceptor sites (blue). b) Distributions of jump time τ_{jump} for water molecules H-bonded to acceptor sites in the hydration shell of both DNA- and RNA- GGGG sequences, decomposed into contributions from water molecules hydrating the sugar (pink), base (red) or phosphate (blue) moieties. Phosphate acceptors are further decomposed into O_R (squares), O_S (circles) and O3′ or O5′ (triangles) atoms. Plots were prepared using Matplotlib,[56] using a bin width of 0.7 ps.

slower hydration dynamics next to phosphate O_R sites in RNA. In A-RNA, water molecules have been found to bridge neighbor phosphate groups, and suggested by simulations to form long-lived water bridges.[1,31,34] In our simulations, successive phosphate O_R oxygen atoms along each strand are indeed bridged by a single water molecule 43% of the time. However,

these water bridges are not responsible for the slow hydration dynamics encountered around the phosphate groups, since the jump dynamics of water molecules initially H-bonded to a phosphate O_R atom are very similar irrespective of whether the second hydrogen atom is H-bonded to the neighbor phosphate group (bridge conformation) or to water (not bridge) (see SI Fig. S10). In other words, the H-bonds formed by a water molecule in bridge between two phosphate groups are not longer lived than those of other water molecules bound to the phosphate O_R. This finding nuances the usual picture of long-lived water bridges between RNA phosphates. However, the location of the "bridging" water molecules is much better defined by the 2 H-bonds with the phosphate backbone compared to singly-bound water molecules, which leads to a higher water density at those specific locations and explains their better resolution in X-ray experiments.[1]

Since the peculiar slowdown at RNA O_R sites is not due to long-lived water bridges, we now use our jump model[55,57] for water reorientation dynamics to identify the physical determinants of the slowdown next to these sites in DNA and RNA, and understand which physical factors cause the split in water reorientation dynamics between the two phosphate oxygen atoms in RNA. Previous works[54,55,57] have shown that the effect of the environment on the jump time can be quantified through two main factors, $\rho = \rho_{TSEV} \times \rho_{TSHB}$ (details in SI). The entropic Transition-State Excluded Volume (TSEV) factor, ρ_{TSEV}, quantifies the slowdown due to the presence of a nearby solute that hinders the approach of the new acceptor. The Transition State Hydrogen Bond (TSHB) factor ρ_{TSHB} describes how the nature and restraints imposed by the solute modulate the free energy cost to elongate the initial H-bond to its transition-state geometry.

The retardation factor predicted by our extended jump model compares well with that effectively observed in our simulations ρ_{jump} (Fig. 3), which demonstrates the validity of the model. While our model slightly underestimates the absolute value of the retardation factor, it captures almost quantitatively (see Table S2) the split in hydration dynamics between the phosphate O_R and O_S atoms, both in RNA and DNA, which is key for our

purpose here. Note that explicitly taking into account the excluded volume coming from background potassium counterions is required in RNA to capture the full extent of the split (see Table S2) and recover a better estimate of the absolute value of the retardation factor, while it has only a very minor impact in DNA. The decomposition into the different molecular factors determining the jump time (Fig. 3) shows that the split in RNA between the hydration dynamics of the two phosphate oxygen atoms originates both from the larger excluded volume next to O_R—coming both from the RNA and the counterions—and from the stronger initial H-bond at this oxygen.

These two effects can be linked to the distinct helical conformations of B-DNA and A-RNA helices, as the orientation of the phosphate groups strongly differs between the two double helical conformations (Figure S1). The phosphate group points away from the helix principal axis in B-DNA, whereas it is more parallel to the axis in A-RNA (see α_{OP2} angle in Figure 4a and b). This results in different orientations of the phosphate oxygen atoms: in DNA, the two oxygen atoms point outside the groove, thus resulting in similar hydration dynamics for the two phosphate oxygens due to similar environments, whereas in RNA, O_R strongly points towards the inside of the groove (see Figure 4a,c,d with very small values of α_{P_R}). This logically results in larger excluded volumes (larger ρ_{TSEV}) at O_R. It also imposes stronger restraints on the elongation of the initial water-phosphate H-bond—the H-bonded water in this case being confined inside the groove— thus leading to a larger ρ_{TSHB}, and overall to a significantly more pronounced slowdown.

In A-RNA, the close proximity of phosphate groups on both sides of the major groove, as visible on Figure 1 and quantified by the width of the RNA major groove—which is even narrower than the DNA minor groove (see SI Figure S3)—also leads to a different structure of the ion cloud around RNA and DNA (see Fig. S13), as already described in previous works.[37,38] In particular, we note in RNA a larger density of K^+ counterions next to the phosphate groups, in the major groove and close the O_R atom. In DNA, the cations are mainly at the bottom of the major groove next to the bases and along the helix principal

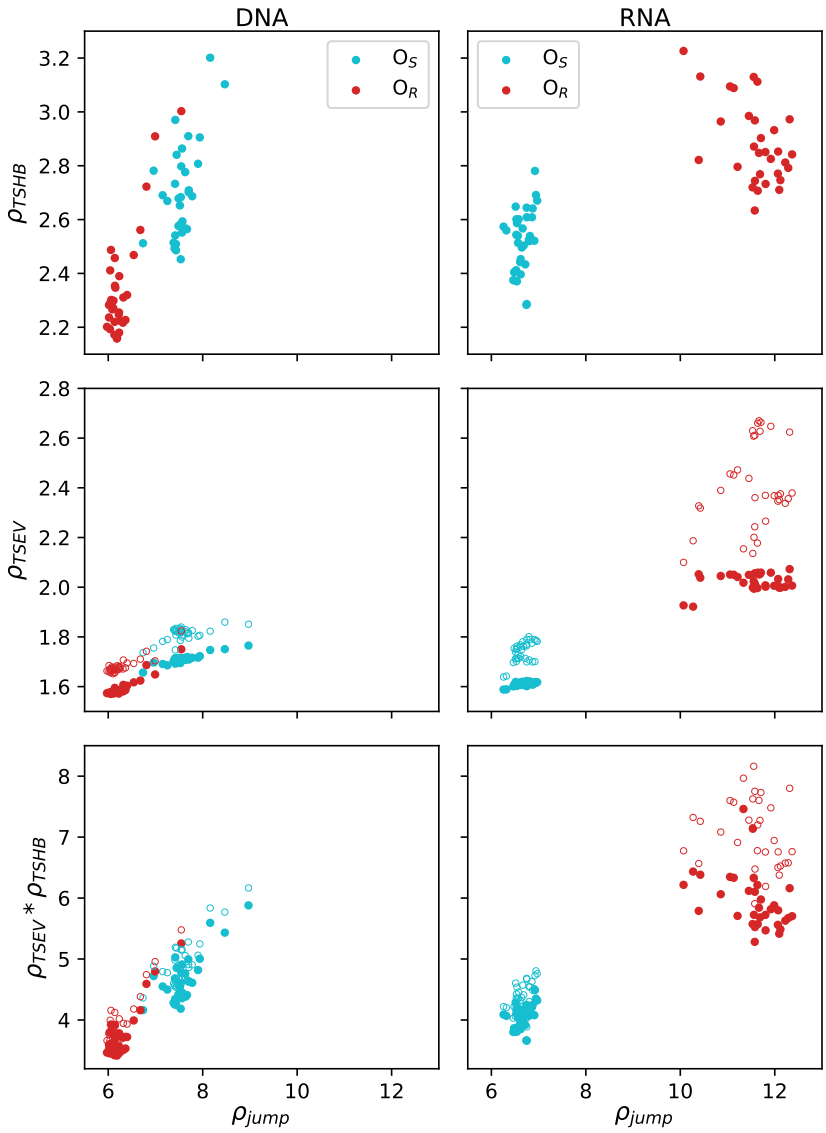

Figure 3: Correlation between the retardation factor for phosphate O_R and O_S atoms, directly computed from jump times (ρ_{jump}), and that predicted with different components of the Extended Jump Model: ρ_{TSHB}, ρ_{TSEV} or $\rho_{TSEV} \times \rho_{TSHB}$. ρ_{TSEV} is calculated taking only into account the nucleic acid excluded volume (filled circles), or included that coming from the ions (empty circles). Plots were prepared using Matplotlib.[56]

axis, with a much smaller density next to the phosphate groups. This explains why inclusion of the excluded volume due to the counterions was necessary to capture the full extent of the slowdown and the split in hydration dynamics between the two phosphate oxygen atoms in RNA, but not in DNA. Note however that the increase of the slowdown due to the ions predicted by our jump model, while noticeable for RNA O_R, remains very modest (factor 1.1

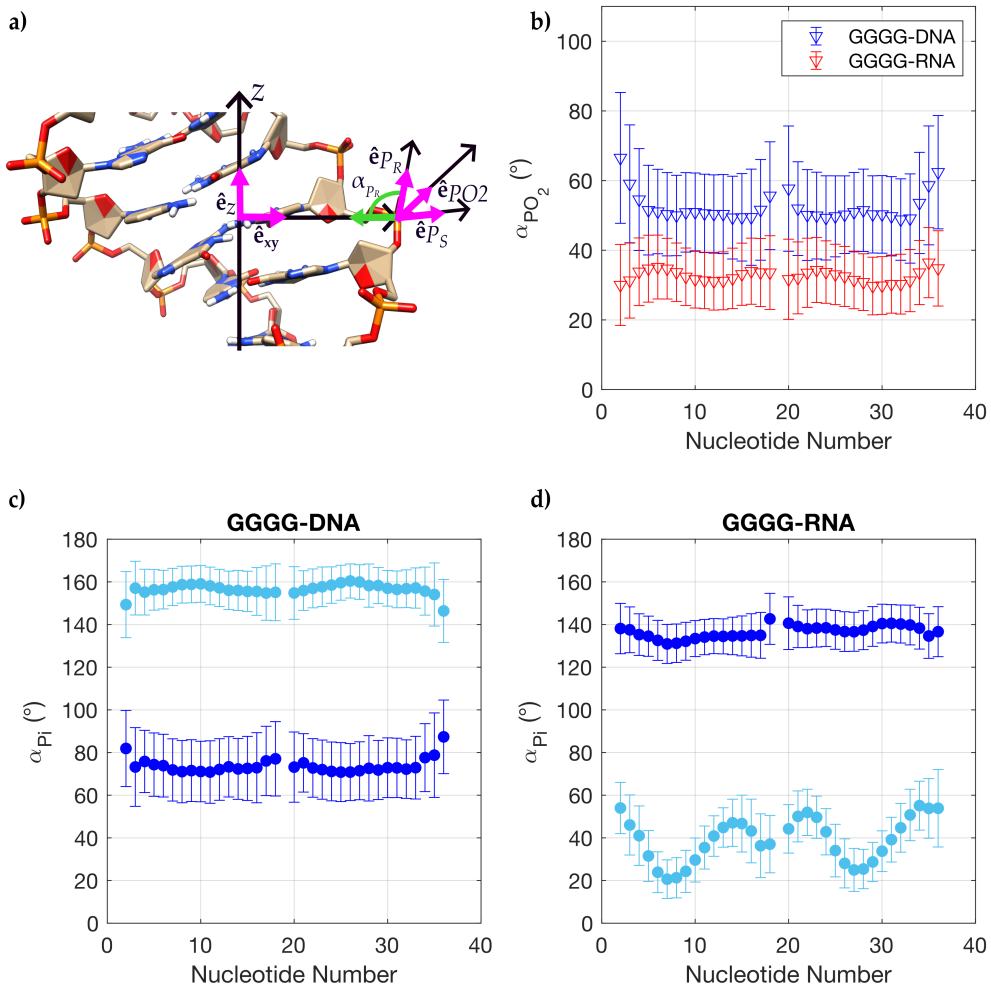

Figure 4: a) Definition of the unit vectors used to define the angles α_{OP2}, α_{P_R} and α_{P_S}. c) Average and standard deviation of the angle α_{OP2} for the GGGG-DNA (blue) and GGGG-RNA (red). Bottom: Average and standard deviation of the angle α_{P_i} for GGGG-DNA (d) and GGGG-RNA (e) (light blue for the angle α_{P_R} and blue for the angle α_{P_S}). The plots were prepared using Matlab.[58]

on average). In addition, the decay of the jump correlation function is independent of the initial presence of a counterion in the water hydration shell (see SI Figure S14), which shows that the memory of the ion presence is lost faster than the typical jump time. Therefore, the presence of slow water molecules cannot be ascribed to that of ions near these locations.

Now that we have rationalized the differences in hydration dynamics at the phosphate

groups, we use our jump model to investigate why the acceptor sites with slow hydration dynamics in the DNA minor groove (cytosine O2, τ_{jump} ∼24–31 ps), have a much faster hydration dynamics in RNA, where they are on the floor of the shallow groove (τ_{jump} ∼9–10 ps) (see SI Figure S15). There, the jump model does not work quantitatively, because it focuses on jumps to (bulk) water, whereas at these confined locations in narrow grooves about half of the jumps occur towards another acceptor site of the biomolecule (see SI for a detailed discussion). However, our model does qualitatively capture the difference in dynamics at these sites between DNA and RNA: $\frac{\rho_{jump}^{DNA}}{\rho_{jump}^{RNA}} \simeq \frac{\rho_{TSEV}^{DNA} \times \rho_{TSHB}^{DNA}}{\rho_{TSEV}^{RNA} \times \rho_{TSHB}^{RNA}} \sim 3$. The larger retardation factor predicted from our jump model at these sites in DNA comes both from a larger excluded volume at these sites ($\rho_{TSEV}^{DNA}/\rho_{TSEV}^{RNA} \sim 1.5$) and from a stronger initial H-bond ($\rho_{TSHB}^{DNA}/\rho_{TSHB}^{RNA} \sim 2$), so that jumps to water acceptors are slowed down. In addition, jumps to nucleic acid acceptor sites (mainly N3(G)) also appear less favored in DNA then RNA. This can also be linked to the different double helical geometries, that position N3(G) a bit further from O2 in B-DNA than A-RNA (on average 4 vs 3.6 Å).

In contrast with this successful determination of the molecular origin of changes in hydration dynamics, the jump model cannot rationalize the slower dynamics observed in DNA at the O2(C) sites on the floor on the minor groove for the GCGC sequence ($\rho_{jump}(GCGC)/\rho_{jump}(GGGG) \simeq 1.3$), as the computed TSEV factor (with or without ions) predicts the reverse ordering ($\rho_{TSEV}(GCGC)/\rho_{TSEV}(GGGG) \simeq 0.8$). This shows the limits of our Jump Model which was not designed to work in such confined and restrained environments. Rationalizing at the molecular level the sequence-dependence at slow sites on the DNA minor groove would deserve additional investigation in future work.

In summary, we obtained an unprecedented high resolution mapping of the hydration dynamics around analogous ds-RNA and ds-DNA 18-mers, which allowed us to highlight, beyond apparently similar features with an average moderate slowdown, key differences. We rationalize these differences and obtain a physical understanding of their molecular determinants thanks to an analytic jump model. In RNA, the slowest water molecules belong to the

phosphate hydration, while they are located close to the bases in the minor groove in DNA. Focusing on phosphate hydration, the two phosphate oxygen atoms O_R and O_S exhibit very distinct dynamics in RNA, which is not the case in DNA. The specific slowdown of O_R hydration is not due to the presence of water molecules bridging successive phosphate groups, that have similar dynamics to that of non bridging hydration water at these sites. Instead, we showed, using our Extended Jump Model, that it is caused in RNA by both a larger excluded volume and a stronger initial H-bond next to O_R. These two factors originate from the markedly different phosphate orientations in RNA, which result from the different double helical conformation of B-DNA and A-RNA. The same framework was used to rationalized the absence of slow sites in the RNA grooves.

While this work has focused on two specific GC-rich sequences, the main features of DNA and RNA hydration dynamics (e.g., heterogeneity and location of fast or slower hydration sites, split of RNA phosphate hydration dynamics, nature of the slowest sites) have been linked to the overall shape of the double helix (A-form vs B-form) rather than to specific chemical features of the bases, so we expect all these observations to be similar in AT/U-rich sequences. The main difference can be expected at slow sites at bases on the floor of the DNA minor groove, where we already see here a difference between GGGG and CGCG sequences. In addition, we know from previous work that AAAA-rich sequences have narrow minor grooves, where we expect much slower hydration dynamics.[13,18,27,28] The dynamics in the grooves could be further sensitive to small changes in helical conformation, that can be experimentally modulated for instance by the background salt concentration and nature,[59] and in simulations can depend on the force field used for water, nucleic acids and ions.[60] Hydration dynamics at these sites and its sequence-dependence will be investigated in future work.

The molecular-level understanding of RNA hydration dynamics provided by such approaches will be important in a number of contexts. These include drug binding and the formation of protein–nucleic acid complexes[12]—key for the regulation of gene expression—as

well as the the formation of RNA–protein biomolecular condensates through liquid/liquid phase separation, as these processes all involve dehydration of the slowest RNA hydration sites, phosphate groups and grooves. Depending on the relative timescale of binding and water dynamics, hydration dynamics can play an important role in those essential biochemical processes.

Acknowledgement

We thank P. Auffinger for stimulating discussions and useful comments on an initial version of this manuscript. This work was supported by the "Initiative d'Excellence" program from the French State (Grants "DYNAMO", ANR-11-LABX-0011, and grant "CACSICE", ANR-11-EQPX-0008). Computational work was performed using HPC resources from GENCI (project A0110711021).

Supporting Information Available

Supporting Information is available, with computational details, additional analyses of the nucleic acid structures and jump times, and ion density maps. All input, parameter files, reorientation and jump maps are shared in a separate archive folder SI-files.zip, as well as on a Zenodo public folder,[61] which also contains the two trajectories GGGG-DNA and GGGG-RNA.

References

(1) Westhof, E. Water: an Integral Part of Nucleic Acid Structure. *Annu. Rev. Biophys. Biophys. Chem.* **1988**, *17*, 125–144.

(2) Miller, M. C.; Buscaglia, R.; Chaires, J. B.; Lane, A. N.; Trent, J. O. Hydration Is a Major

Determinant of the G-Quadruplex Stability and Conformation of the Human Telomere 3′ Sequence of d($AG_3(TTAG_3)_3$). *J. Am. Chem. Soc.* **2010**, *132*, 17105–17107.

(3) Saenger, W.; Hunter, W. N.; Kennard, O. DNA Conformation Is Determined by Economics in the Hydration of Phosphate Groups. *Nature* **1986**, *324*, 385–388.

(4) Csaszar, K.; Špačková, N.; Štefl, R.; Šponer, J.; Leontis, N. B. Molecular Dynamics of the Frame-Shifting Pseudoknot from Beet Western Yellows Virus: The Role of Non-Watson-Crick Base-Pairing, Ordered Hydration, Cation Binding and Base Mutations on Stability and Unfolding. *J. Mol. Biol.* **2001**, *313*, 1073–1091.

(5) Reblová, K.; Špačková, N.; Stefl, R.; Csaszar, K.; Koča, J.; Leontis, N. B.; Šponer, J. Non-Watson-Crick Basepairing and Hydration in RNa Motifs: Molecular Dynamics of 5S rRNA Loop E. *Biophys. J.* **2003**, *84*, 3561–3582.

(6) Krasovska, M. V.; Sefcikova, J.; Réblová, K.; Schneider, B.; Walter, N. G.; Šponer, J. Cations and Hydration in Catalytic RNA: Molecular Dynamics of the Hepatitis Delta Virus Ribozyme. *Biophys. J.* **2006**, *91*, 626–638.

(7) Špačková, N.; Šponer, J. Molecular Dynamics Simulations of Sarcin-Ricin rRNA Motif. *Nucleic Acids Res.* **2006**, *34*, 697–708.

(8) Rhodes, M. M.; Réblová, K.; Šponer, J.; Walter, N. G. Trapped Water Molecules Are Essential to Structural Dynamics and Function of a Ribozyme. *P. Natl. Acad. Sci. USA* **2006**, *103*, 13380–13385.

(9) Auffinger, P.; Hashem, Y. Nucleic Acid Solvation: From Outside to Insight. *Cur. Opin. Struct. Biol.* **2007**, *17*, 325–333.

(10) Pal, S. K.; Zewail, A. H. Dynamics of Water in Biological Recognition. *Chem. Rev.* **2004**, *104*, 2099–2124.

(11) Jayaram, B.; Jain, T. The Role of Water in Protein-DNA Recognition. *Annu. Rev. Biophys. Biomol. Struct.* **2004**, *33*, 343–361.

(12) Corley, M.; Burns, M. C.; Yeo, G. W. How RNA-Binding Proteins Interact with RNA: Molecules and Mechanisms. *Molecular Cell* **2020**, *78*, 9–29.

(13) Drew, H. R.; Dickerson, R. E. Structure of a B-DNA Dodecamer. *J. Mol. Biol.* **1981**, *151*, 535–556.

(14) Shui, X.; McFail-Isom, L.; Hu, G. G.; Williams, L. D. The B-DNA Dodecamer at High Resolution Reveals a Spine of Water on Sodium. *Biochemistry* **1998**, *37*, 8341–8355.

(15) Bastos, M.; Castro, V.; Mrevlishvili, G.; Teixeira, J. Hydration of ds-DNA and ss-DNA by Neutron Quasielastic Scattering. *Biophys. J.* **2004**, *86*, 3822–3827.

(16) Liepinsh, E.; Otting, G.; Wuthrich, K. NMR Observation of Individual Molecules of Hydration Water Bound to DNA Duplexes: Direct Evidence for a Spine of Hydration Water Present in Aqueous Solution. *Nucleic Acids Res.* **1992**, *20*, 6549–6553.

(17) Zhou, D.; Bryant, Robert G. Water Molecule Binding and Lifetimes on the DNA Duplex $d(CGCGAATTCGCG)_2$. *J. Biomol. NMR* **1996**, *8*, 77–86.

(18) Denisov, V. P.; Carlström, G.; Venu, K.; Halle, B. Kinetics of DNA Hydration. *J. Mol. Biol.* **1997**, *268*, 118–136.

(19) Franck, J. M.; Ding, Y.; Stone, K.; Qin, P. Z.; Han, S. Anomalously Rapid Hydration Water Diffusion Dynamics Near DNA Surfaces. *J. Am. Chem. Soc.* **2015**, *137*, 12013–12023.

(20) Pal, S. K.; Zhao, L.; Zewail, A. H. Water at DNA Surfaces: Ultrafast Dynamics in Minor Groove Recognition. *P. Natl. Acad. Sci. USA* **2003**, *100*, 8113–8.

(21) Andreatta, D.; Pérez Lustres, J. L.; Kovalenko, S. A.; Ernsting, N. P.; Murphy, C. J.; Coleman, R. S.; Berg, M. A. Power-Law Solvation Dynamics in DNA over Six Decades in Time. *J. Am. Chem. Soc.* **2005**, *127*, 7270–7271.

(22) Szyc, Ł.; Yang, M.; Nibbering, E. T. J.; Elsaesser, T. Ultrafast Vibrational Dynamics and Local Interactions of Hvdrated DNA. *Angewandte Chemie* **2010**, *49*, 3598–3610.

(23) Chuprina, V. P.; Heinemann, U.; Nurislamov, A. A.; Zielenkiewicz, P.; Dickerson, R. E.; Saenger, W. Molecular Dynamics Simulation of the Hydration Shell of a B-DNA Decamer Reveals Two Main Types of Minor-Groove Hydration Depending on Groove Width. *Proc. Natl. Acad. Sci. U.S.A.* **1991**, *88*, 593–597.

(24) Bonvin, A. M. J. J.; Sunnerhagen, M.; Otting, G.; Van Gunsteren, W. F. Water Molecules in DNA Recognition II: a Molecular Dynamics View of the Structure and Hydration of the Trp Operator. *J. Mol. Biol.* **1998**, *282*, 859–873.

(25) Pal, S.; Maiti, P. K.; Bagchi, B.; Hynes, J. T. Multiple Time Scales in Solvation Dynamics of DNA in Aqueous Solution: the Role of Water, Counterions, and Cross-Correlations. *J. Phys. Chem. B* **2006**, *110*, 26396–26402.

(26) Yonetani, Y.; Kono, H. Sequence Dependencies of DNA Deformability and Hydration in the Minor Groove. *Biophys. J.* **2009**, *97*, 1138–1147.

(27) Saha, D.; Supekar, S.; Mukherjee, A. Distribution of Residence Time of Water Around DNA Base Pairs: Governing Factors and the Origin of Heterogeneity. *J. Phys. Chem. B* **2015**, *119*, 11371–11381.

(28) Duboué-Dijon, E.; Fogarty, A. C.; Hynes, J. T.; Laage, D. Dynamical Disorder in the DNA Hydration Shell. *J. Am. Chem. Soc.* **2016**, *138*, 7610–7620.

(29) Westhof, E.; Dumas, P.; Moras, D. Hydration of Transfer RNA Molecules: A Crystallographic Study. *Biochimie* **1988**, *70*, 145–165.

(30) Dock-Bregeon, A.; Chevrier, B.; Podjarny, A.; Johnson, J.; de Bear, J. S.; Gough, G.; Gilham, P.; Moras, D. Crystallographic Structure of an RNA Helix: $[U(UA)_6A]_2$. *J. Mol. Biol.* **1989**, *209*, 459–474.

(31) Egli, M.; Portmann, S.; Usman, N. RNA Hydration: A Detailed Look. *Biochemistry* **1996**, *35*, 8489–8494.

(32) Bolton, P.; Kearns, D. Hydrogen Bonding of the 2′ OH in RNA. *BBA - Nucl. Acids Prot. Synth.* **1978**, *517*, 329–337.

(33) Conte, M. R.; Conn, G. L.; Brown, T.; Lane, A. N. Hydration of the RNA Duplex r(CGCAAAUUUGCG)$_2$ Determined by NMR. *Nucleic Acids Res.* **1996**, *24*, 3693–3699.

(34) Auffinger, P.; Westhof, E. RNA Hydration: Three Nanoseconds of Multiple Molecular Dynamics Simulations of the Solvated tRNA(Asp) Anticodon Hairpin. *J. Mol. Biol.* **1997**, *269*, 326–341.

(35) Auffinger, P.; Westhof, E. Hydration of RNA Base Pairs. *J. Biomol. Struct. Dyn.* **1998**, *16*, 693–707.

(36) Auffinger, P.; Westhof, E. RNA Solvation: A Molecular Dynamics Simulation Perspective. *Biopolymers* **2000**, *56*, 266–274.

(37) Auffinger, P.; Westhof, E. Water and Ion Binding Around RNA and DNA (C,G) Oligomers. *J. Mol. Biol.* **2000**, *300*, 1113–1131.

(38) Auffinger, P.; Westhof, E. Water and Ion Binding Around r(UpA)$_{12}$ and d(TpA)$_{12}$ Oligomers - Comparison with RNA and DNA (CpG)$_{12}$ Duplexes. *J. Mol. Biol.* **2001**, *305*, 1057–1072.

(39) Yoon, J.; Lin, J. C.; Hyeon, C.; Thirumalai, D. Dynamical Transition and Heterogeneous Hydration Dynamics in RNA. *J. Phys. Chem. B* **2014**, *118*, 7910–7919.

(40) Lammert, H.; Wang, A.; Mohanty, U.; Onuchic, J. N. RNA As a Complex Polymer with Coupled Dynamics of Ions and Water in the Outer Solvation Sphere. *J. Phys. Chem. B* **2018**, *122*, 1–27.

(41) Rázga, F.; Zacharias, M.; Réblová, K.; Koča, J.; Šponer, J. RNA Kink-Turns As Molecular Elbows: Hydration, Cation Binding, and Large-Scale Dynamics. *Structure* **2006**, *14*, 825–835.

(42) Pasi, M.; Maddocks, J. H.; Beveridge, D.; Bishop, T. C.; Case, D. A.; Cheatham, I., Thomas; Dans, P. D.; Jayaram, B.; Lankas, F.; Laughton, C. et al. μABC: A Systematic Microsecond Molecular Dynamics Study of Tetranucleotide Sequence Effects in B-DNA. *Nucleic Acids Res.* **2014**, *42*, 12272–12283.

(43) Pérez, A.; Marchán, I.; Svozil, D.; Sponer, J.; Cheatham, T. E.; Laughton, C. A.; Orozco, M. Refinement of the AMBER Force Field for Nucleic Acids: Improving the Description of α/γ Conformers. *Biophys. J.* **2007**, *92*, 3817–3829.

(44) Zgarbová, M.; Otyepka, M.; Šponer, J.; Mládek, A.; Banáš, P.; Cheatham, T. E.; Jurečka, P. Refinement of the Cornell et Al. Nucleic Acids Force Field Based on Reference Quantum Chemical Calculations of Glycosidic Torsion Profiles. *J. Chem. Theory Comput.* **2011**, *7*, 2886–2902.

(45) Berendsen, H. J. C.; Grigera, J. R.; Straatsma, T. P. The Missing Term in Effective Pair Potentials. *J. Phys. Chem.* **1987**, *91*, 6269–6271.

(46) Humphrey, W.; Dalke, A.; Schulten, K. VMD: Visual Molecular Dynamics. *J. Mol. Graphics* **1996**, *14*, 33–38.

(47) Fogarty, A. C.; Laage, D. Water Dynamics in Protein Hydration Shells: the Molecular Origins of the Dynamical Perturbation. *J. Phys. Chem. B* **2014**, *118*, 7715–7729.

(48) Duboué-Dijon, E.; Laage, D. Comparative Study of Hydration Shell Dynamics Around a Hyperactive Antifreeze Protein and Around Ubiquitin. *J. Chem. Phys.* **2014**, *141*, 22D529.

(49) Laage, D.; Hynes, J. T. On the Residence Time for Water in a Solute Hydration Shell: Application to Aqueous Halide Solutions. *J. Phys. Chem. B* **2008**, *112*, 7697–7701.

(50) Abragam, A. *The Principles of Nuclear Magnetism.*; Oxford: UK: Clarendon, 1961.

(51) Laage, D.; Hynes, J. T. A Molecular Jump Mechanism of Water Reorientation. *Science* **2006**, *311*, 832–835.

(52) Laage, D.; Hynes, J. T. On the Molecular Mechanism of Water Reorientation. *J. Phys. Chem. B* **2008**, *112*, 14230–14242.

(53) Fisette, O.; Päslack, C.; Barnes, R.; Isas, J. M.; Langen, R.; Heyden, M.; Han, S.; Schäfer, L. V. Hydration Dynamics of a Peripheral Membrane Protein. *J. Am. Chem. Soc.* **2016**, *138*, 11526–11535.

(54) Fabio Sterpone; Stirnemann, G.; Laage, D. Magnitude and Molecular Origin of Water Slowdown Next to a Protein. *J. Am. Chem. Soc.* **2012**, *134*, 4116–4119.

(55) Fogarty, A. C.; Duboué-Dijon, E.; Sterpone, F.; Hynes, J. T.; Laage, D. Biomolecular Hydration Dynamics: A Jump Model Perspective. *Chem. Soc. Rev.* **2013**, *42*, 5672–5683.

(56) Hunter, J. D. Matplotlib: a 2D Graphics Environment. *Comput. Sci. Eng.* **2007**, *9*, 90–95.

(57) Laage, D.; Stirnemann, G.; Sterpone, F.; Rey, R.; Hynes, J. T. Reorientation and Allied Dynamics in Water and Aqueous Solutions. *Annu. Rev. Phys. Chem.* **2011**, *62*, 395–416.

(58) Inc., T. M. MATLAB Version: 9.13.0 (R2022a). The MathWorks Inc., 2022.

(59) Chen, Y.-L.; Pollack, L. Salt Dependence of A-Form RNA Duplexes: Structures and Implications. *J. Phys. Chem. B* **2019**, *123*, 9773–9785.

(60) Kührová, P.; Mlýnský, V.; Otyepka, M.; Šponer, J.; Banáš, P. Sensitivity of the RNA Structure to Ion Conditions As Probed by Molecular Dynamics Simulations of Common Canonical RNA Duplexes. *J. Chem. Inf. Model.* **2023**, *63*, 2133–2146.

(61) Zenodo Dataset DOI:10.5281/Zenodo.10647894.